Supporting Information

Surface Lattice Resonances for Enhanced and Directional Electroluminescence at High Current Densities

Yuriy Zakharko[†,‡], Martin Held[†,‡], Arko Graf[‡], Tobias Rödlmeier[§,#], Ralph Eckstein[§,#], Gerardo Hernandez-Sosa[§,#], Bernd Hähnlein[||], Jörg Pezoldt[||], and Jana Zaumseil[,‡].*

[‡] Institute for Physical Chemistry, Universität Heidelberg, D-69120 Heidelberg, Germany

[§] Light Technology Institute, Karlsruhe Institute of Technology, D-76131 Karlsruhe, Germany

[#] InnovationLab, Speyerer Straße 4, 69115 Heidelberg, Germany

[||] Institut für Mikro- und Nanotechnologie, Technische Universität Ilmenau, D-98693 Ilmenau, Germany

[†] These authors contributed equally to this work.

Corresponding Author

* E-mail: *zaumseil@uni-heidelberg.de*

1. Methods

Sample fabrication, characterization and simulation

2. Results

1. Methods

LEFET fabrication

Electron-beam lithography (EBL) of the gold nanodisks (NDs) was performed on glass (Schott AF32 Eco) with a Raith 150 system (Raith GmbH). To avoid charging and to allow charge transport from back-scattered electrons, a 2 nm chromium layer was applied via physical vapor deposition (PVD) on top of the glass substrate. Subsequently a two-layer resist consisting of poly(methyl methacrylate) (PMMA) AllResist AR-P 617.03 (90 nm) and AR-P 679.02 (70 nm) was spincoated. The use of a two-layer resist enables an undercut, which is controlled by the annealing temperature (200 °C / 10 min for the AR-P 617.03 and 150 °C / 3 min for the AR-P 679.02). An additional 3 nm gold layer was sputtered on top to avoid charging. EBL was done by exposure in two steps with 10 kV and 60 µm aperture. The first step included the fabrication of alignment markers on which, in the second step, the focus plane was adjusted, which enabled exposure of larger structures in contrast to focusing on the gold surface. After each of the two EBL steps 25 nm gold were applied using PVD. To enhance the adhesive strength the sample was sputtered with argon for 30 s at 100 W before metal deposition. The lift-off process was carried out using dimethylsulphoxide. The structures were oxidized in a rapid thermal annealing process at 500 °C for 30 s. The chromium layer was fully oxidized and had no impact on the plasmonic structure.

To form a thin aluminum oxide layer on top of the NDs, 1 nm of aluminium was evaporated and left to oxidize in air. Photolithography, electron-beam evaporation of 2 nm Cr/30 nm Au and lift-off was employed to pattern the source-drain electrodes with a channel length of 20 µm and width of 500 µm around the ND array.

An 8 mg/mL solution of the light-emitting, high-mobility copolymer DPPT-BT (poly(2,5-bis(2-octyldodecyl)-3,6-di(thiophen-2-yl)diketopyrrolo[3,4-*c*]pyrrole-1,4-dione-*alt*-benzo[*c*][1,2,5]-thiadiazole), M_n = 33 kg/mol, M_w = 87 kg/mol, Flexink Ltd) in chlorobenzene was spincoated at 2000 rpm for 60 s and annealed at 200 °C in dry nitrogen for 30 min, resulting in a 40 nm layer.

The hybrid dielectric consisted of three layers: PMMA, hafnium oxide (HfOx) and aluminium oxide (AlO_x). A syndiotactic PMMA by Polymer Source (M_w = 300 kg/mol) was dissolved in anhydrous n-butyl acetate (50 mg/mL) and heated at 80 °C for 30 min. The PMMA layer was spincoated at 4000 rpm for 60 s, resulting in a film thickness of 226 nm. A 38 nm HfO_x layer was added by atomic layer deposition (Ultratech Savannah S100) using tetrakis(dimethylamino)hafnium as a hafnium precursor at 100 °C and water as an oxygen source. HfO_x acted as an encapsulation barrier to stop the diffusion of H_2O from the PEDOT:PSS to the interface of PMMA and DPPT-BT. To prevent the etching of HfO_x by PEDOT:PSS, a thin AlO_x layer was deposited by ALD with trimethylaluminium as an aluminium precursor and water at 80 °C.

The conductive polymer PEDOT:PSS was used for the gate electrode. A pH-neutral high conductivity PEDOT:PSS dispersion (Sigma Aldrich, Orgacon N-1005, 0.83% in H_2O) with a small addition of Triton-X-100 surfactant (Sigma Aldrich) was printed by an Optomec Aerosol Jet Printer (carrier gas flow 25-30 ccm, sheeth gas flow 6-8 ccm, stage temperature 60 °C, nozzle speed 5 mm/s, line pitch 20 µm), yielding a film thickness of approximately 200 nm. The pH-neutral PEDOT:PSS did not etch the underlying dielectric layer. To avoid additional degradation, all devices were encapsulated for optoelectronic measurements with a glass cover slip and epoxy resin.

Characterization

Current-voltage characteristics were recorded with an Agilent 4156C Semiconductor Parameter Analyzer or a Keithley 2612A source meter. Gate dielectric capacitances were determined with an Agilent E4980A Precision LCR Meter. The absorption spectrum of the DPPT-BT thin film was recorded with a Cary 6000i UV/Vis/NIR absorption spectrometer (Varian).

For angle- and wavelength-dependent spectroscopy, we used a Fourier-space imaging setup, as reported recently.[1] Briefly, for the reflectance or photoluminescence spectroscopy, a collimated white light source or laser beam (λ=785 nm; continuous wave power 5 mW) was passed through a 50:50 beam-splitter and then focused on the sample by a ×100 near IR objective with 0.8 numerical aperture. The back-focal plane of the objective was imaged via Fourier optics and a tube lens onto the entrance slit of a spectrometer (IsoPlane SCT-320, Princeton Instruments) equipped with a cooled 2D InGaAs camera (640×512 pixels NIRvana 640ST, Princeton Instruments). An additional polarizer was placed in front of the spectrometer to select transverse-electric or transverse-magnetic light polarization. The same setup was used to acquire angle-dependent electroluminescence spectra. All spectra were corrected against the response of the detection system with a calibrated tungsten halogen lamp. The electroluminescence image of the emission zone was recorded with the same setup but with the Fourier optics removed and the grating being replaced by a mirror in the spectrometer.

3D Finite-difference time-domain calculations

3D finite-difference time-domain (FDTD) simulations were performed using commercial software (FDTD Solution v8.15.697, Lumerical Solutions Inc., Canada). A uniform mesh size of 2 nm (X, Y and Z-directions) was used in the region ($X \times Y \times Z = 670 \times 400 \times 670$ nm^3) around gold ND. Outside of these regions the grid was defined by the auto non-uniform mesh technique. The optical constants of gold and silver were taken from Johnson and Christy.[2] The complex dielectric constant of the DPPT-BT was taken from reference 3.

The simulation region (boundaries defined by periodic conditions and perfectly matched layers) includes the glass substrate, a thin 40 nm DPPT-BT layer covering gold NDs (h=25 nm, D=300 nm), 226 nm of PMMA with n=1.5, 38 nm HfO_x (n=2), 5 nm AlO_x (n=1.75) and 200 nm PEDOT:PSS (n=1.44). To reduce computational resources and computational time, we took advantage of the symmetric/antisymmetric boundary conditions when possible.

In order to estimate field intensity enhancement profiles we recorded electromagnetic fields with 2D profile monitors. Field intensity enhancement $|Ez/E0|^2$ was calculated for a plane wave injected normal to the surface (Z-polarized) taking into account the values for the configuration without gold NDs. The peak position for the surface lattice resonance was around λ=1350 nm, while experimental values are around λ=1200 nm. The discrepancy is most likely caused by the small variations of the dielectric constant of the environment (and DPPT-BT in particular) that in turn influences the position of the local plasmon resonance of NDs, and thus surface lattice resonance. Nevertheless, qualitatively the mode profiles should not be distorted significantly.

1. Results

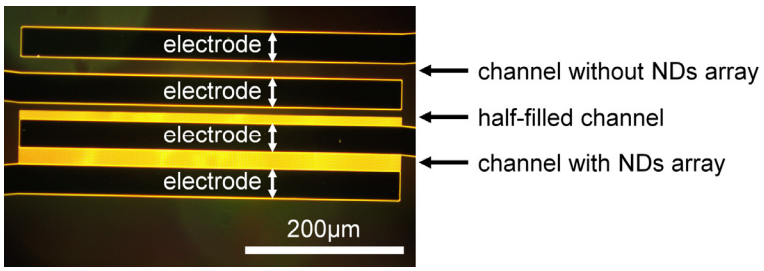

Figure S1. Dark-field microscopy image of LEFET under white-light illumination showing four electrodes and three channels: without, half-covered and with ND array.

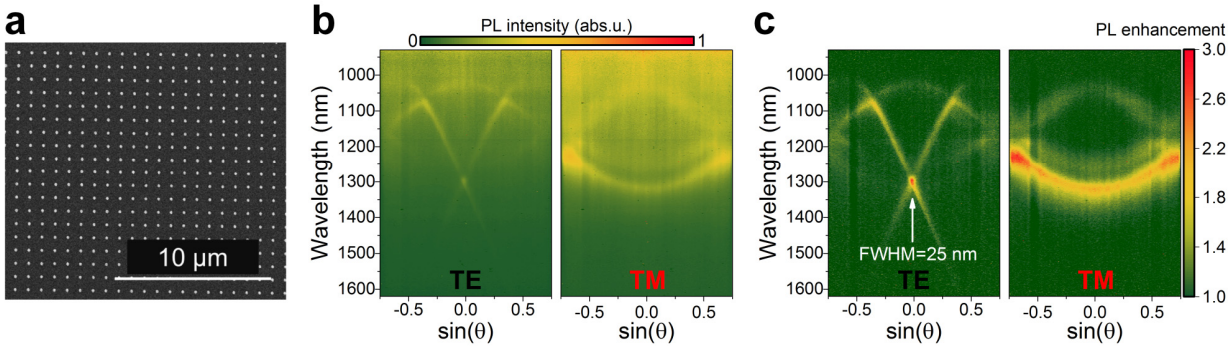

Figure S2. (a) Scanning electron micrograph of periodic array of gold NDs (830 nm pitch and diameter 180-200 nm). Angle- and polarization-resolved (b) photoluminescence and (c) photoluminescence enhancement spectra revealing narrow (full width at half maximum = 25 nm) surface lattice resonances.

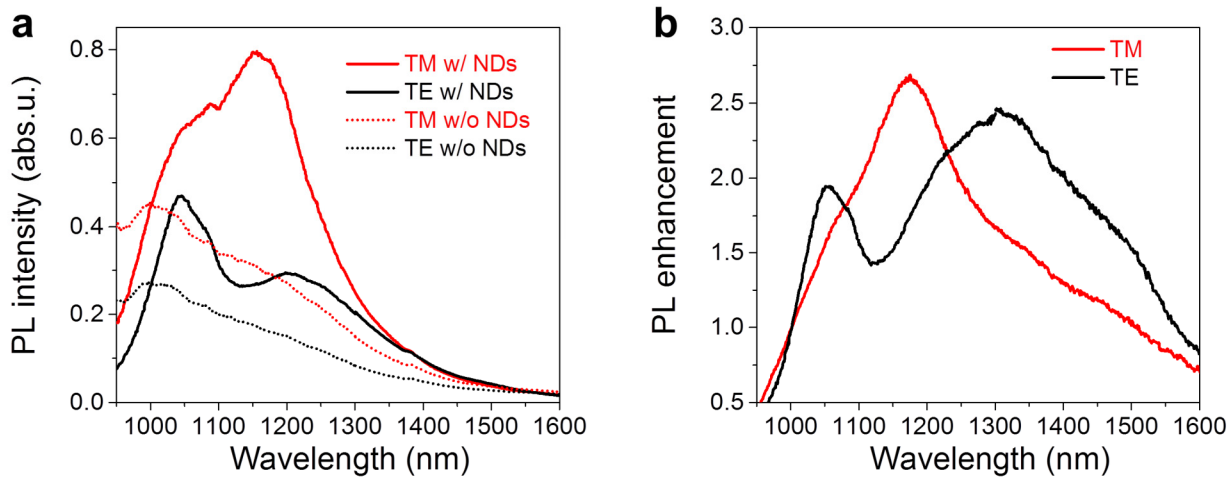

Figure S3. (a) Angle-integrated TE (black) and TM-polarized (red) photoluminescence intensity of the DPPT-BT without (dotted line) and with (solid) 670 nm pitch periodic array of gold NDs. (b) Corresponding photoluminescence enhancement values. Quenching of the signal (i.e enhancement lower than unity) below 1000 nm is due to the increased self-absorption as discussed previously.[3]

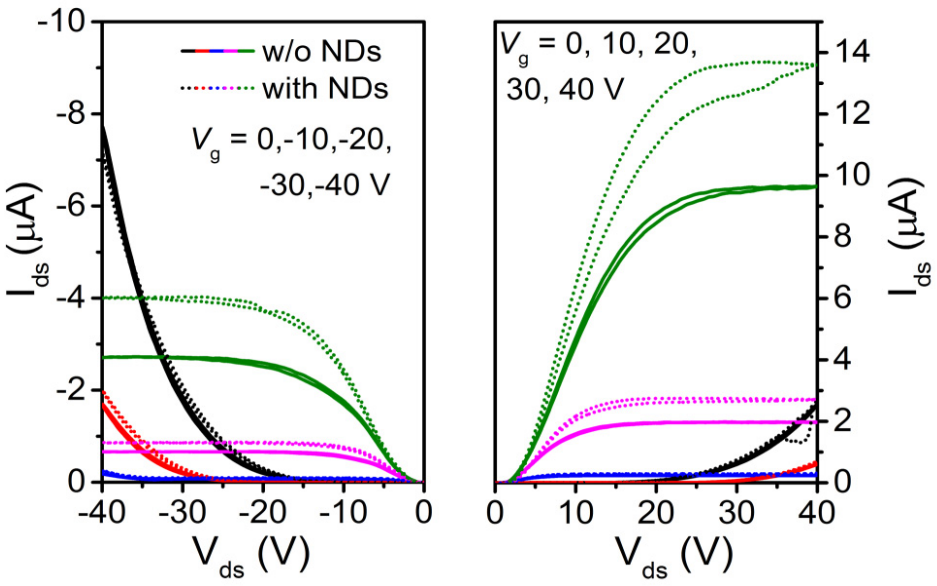

Figure S4. Comparison of ambipolar output characteristics of LEFETs with and without ND array.

Table S5. Charge transport parameters (saturation mobility μ_{sat} and threshold voltages V_{Th} for holes and electrons) extracted from LEFETs with and without ND array in the channel.

	$\mu_{sat,h}$ ($cm^2V^{-1}s^{-1}$)	$V_{Th,h}$ (V)	$\mu_{sat,e}$ ($cm^2V^{-1}s^{-1}$)	$V_{Th,e}$ (V)
without ND array	0.19	-29.6	0.27	23.4
with ND array	0.11	-21.1	0.059	20.7

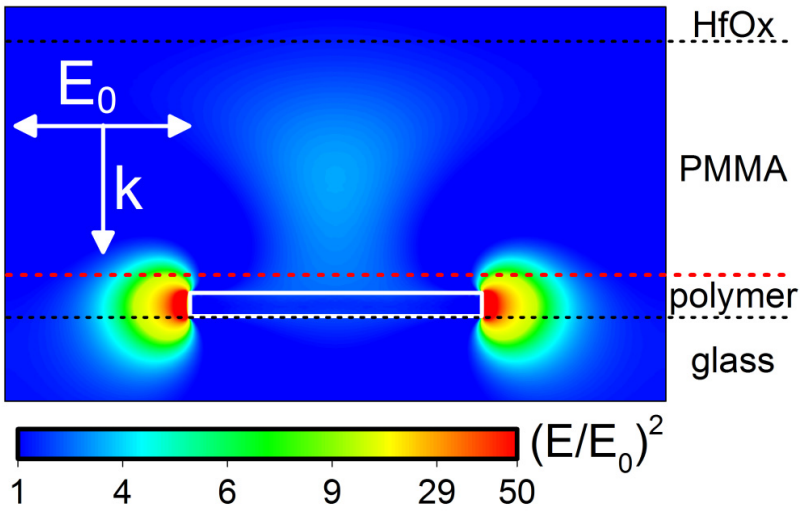

Figure S6. Simulated field intensity enhancement (side view) around ND (white line). Photo-excited excitons recombine across the whole polymer layer, whereas electrically-pumped excitons are only formed at the interface marked with a red dashed line.

REFERENCES

(1) Zakharko, Y.; Graf, A.; Schießl, S. P.; Hähnlein, B.; Pezoldt, J.; Gather, M. C.; Zaumseil, J. Broadband Tunable, Polarization-Selective and Directional Emission of (6,5) Carbon Nanotubes Coupled to Plasmonic Crystals. *Nano Lett.* **2016**, *16*, 3278–3284.

(2) Johnson, P. B.; Christy, R. W. Optical Constants of the Noble Metals. *Phys. Rev. B* **1972**, *6*, 4370–4379.

(3) Zakharko, Y.; Held, M.; Sadafi, F.-Z.; Gannott, F.; Mahdavi, A.; Peschel, U.; Taylor, R. N. K.; Zaumseil, J. On-Demand Coupling of Electrically Generated Excitons with Surface Plasmons via Voltage-Controlled Emission Zone Position. *ACS Photonics* **2016**, *3*, 1–7.